J-Researchers

JOURNAL OF CIVIL ENGINEERING RESEARCHERS

Study on the Performance of High-Strength Steel Shear Wall with Opening and Pre-crack

Mohammad komeil Sadeghi golafshani [a,*]

[a] Department of Civil Engineering, Chalous Branch, Islamic Azad University, Chalous, Iran

Article History: Received date 2022.08.31; revised date : 2022.08.11; accepted 2022.09.12

Abstract

The use of steel shear wall in engineering construction, including high-rise building projects that bear high lateral forces, is of great importance and practical. Since the steel shear wall with opening may have some pre-cracks due to initial damage and cause the weak lateral behavior of the shear wall, in this study, the simultaneous impact of pre-crack and opening in the three-story and one-span frame with steel shear wall has been evaluated. In this study, 48 numerical samples have been studied using the finite element method and Abaqus software. Axial and lateral loading has been applied to the samples, and the parameters of the pre-crack position, pre-crack length and the type of shear wall steel sheet material have been investigated. The results of this study demonstrated that the numerical model made for the shear wall provides reliable answers compared to the laboratory model. In the shear walls under study, the parameter of crack length and crack position has a high impact on the ductility capacity, while it has little impact on the hardness and strength index. The most critical pre-crack modes in the horizontal position, located at the top or bottom corner of the frame, have had a great impact on the lateral behavior and reduced ductility by 60% and wall strength by 32%. On the other hand, by changing the materials of the shear wall steel sheet from LYP steel to St37 and St52, the final strength and hardness have increased by 3.63 and 1.45 times, respectively and the ductility has decreased by30%. (DOI:https//doi.org/10.52547/JCER.4.2.22)

Keywords: steel shear wall, circular opening, horizontal and vertical pre-crack, axial-lateral loading, finite performance

* Corresponding author. Tel.: +98 912 021 2987; E-mail: mk.sadeghi92@gmail.com

1. Introduction

The steel plate shear wall (SPSW) system is a type of lateral force resisting structure that consists of filling plates and boundary elements. SPSWs offer quick installation and easy production standardization. In a study, Thorburn [1] showed that a thin steel plate after buckling forms a tensile field that can continue to resist horizontal load. The postbuckling performance of thin SPSWs has attracted the attention of researchers. In another study, Elgaaly [2] and Caccese [3] found that out-of-plane buckling occurs in thin SPSW under a small shear load and a "pinching" phenomenon appears in the hysteresis curve. In general, stiffeners are placed to steel plates in order to improve their performance. The common shapes of stiffeners in common shear walls with openings include cross stiffeners, diagonal stiffeners, multiple stiffeners, etc. [4,5] which have been evaluated in previous studies. Chen [6] investigated the elastic buckling behavior and hysteresis behavior of stiffened SPSWs. The results indicate that the elastic buckling load is linearly related to the bending stiffness of diagonal stiffeners that diagonally have been reinforced with stiffeners and SPSWs and have better bearing capacity and hysteresis performance than SPSWs with cross stiffeners. Guo [7] in a different research showed that semi-rigid connections weaken the overall stability of the structure and change the distribution of forces and bending moments of the connections. Sigariyazd [8] conducted one-way static pushover tests on a diagonally stiffened SPSW and a slanted stiffener SPSW, studied the effect of slanted stiffeners on the bearing capacity, and presented a theoretical formula for calculating the bearing capacity.

In another study, Alavi [9,10] suggested that a channel-shaped stiffener with high torsional stiffness can be used as a more effective stiffener. Du [11] and Deng [12] used a multi-crenation network of channels and a diagonal channel to repair damaged SPSW. Channel stiffeners effectively repaired the damaged plate and reduced the tension field effect. Tong [13] investigated the elastic buckling behavior of trapezoidal-corrugated SPSW with vertical stiffener. Xu [14] and Tong [15] proposed stiffness formulas for vertical channel stiffened plate under shear or compression loading.

In a study, Nie [16] tested SPSWs with a vertical channel stiffener having openings. The results show that the opening can reduce the stiffness and bearing capacity of the structure, and by placing the stiffener at the edge of the opening, the stability of the structure increases. Hosseinzadeh [17] conducted a nonlinear numerical analysis of a SPSW with large rectangular openings and stiffeners. In various stiffened perforated structures, the stiffened open edge can increase both ultimate strength and stiffness while slightly reducing the ductility ratio. Sabouri Ghomi [18] evaluated the impact of two openings on the structural behavior of SPSWs. Opening distance had little effect on lateral bearing capacity, stiffness and energy absorption. However, the opening caused the depression of these numbers. Shekastehband [19] studied the seismic behavior of a SPSW with fully connected John plates and only beams. The ductility ratio of the structure can be improved only when connected to beams, but the energy dissipation capacity and shear strength of the structure are clearly lower than those of fully connected John plates. To study the effect of different opening shapes and hardening shapes on the hysteresis behavior of SPSWs, two samples with a scale of 1 to 3 were designed. A sample was reinforced SPSW with a diagonal channel and two rectangular openings. The other was a stiffened SPSW inclined channel with a rectangular opening.

Since steel panels can have considerable strength and stiffness, they may sometimes impose a greater share of floor shears on boundary columns, which may lead to their premature failure. Attempts to reduce the columns demand in SPSWs have recently been made using cold-rolled steel panels, [20] the use of LYP steel plates, [21-22] the use of perforated John plates with regular circular holes [23] and the use of semi-supported steel shear walls (SSSWs) [24-25] have been proposed. Shekastehband et al. [26] studied the effects of hole diameter as well as slenderness ratios of John plates on the seismic behavior of SSSWs. Based on the test results, the strength, stiffness, ductility coefficient and energy absorption characteristics of the samples were significantly reduced in the samples with openings. Wei et al. [27] investigated a series of new semi-connected SPSWs. The results of the proposed test showed that the proposed SPSW demonstrates good structural performance in terms of initial stiffness, shear strength, ductility, and energy absorption capability.

In this article, 48 samples of steel frames with circular openings and pre-cracks have been simulated

using the finite element method and quasi-static analysis. Bearing capacity, pushover behavior, ductility, damage of the samples are presented.

2. Finite Element Method

Laboratory studies are the most effective method for research in the field of structural behavior which becomes important due to the expensive and time-consuming nature of numerical studies. Many studies have been conducted in the field of steel shear wall. The results of using the numerical method for these studies show that the ABAQUS [28] software has a good performance in the responses of non-linear behavior of materials and hysteresis diagrams. In order to study more on the behavior of unstiffened thin steel shear wall structures, an efficient and accurate finite element method should be proposed. The steel sheet shear wall structure consists of beams, columns, steel filler panel and connection plates. Past studies proved that residual stress has little effect on the shear wall behavior of steel sheet, which can be neglected in the modeling process. Beam, column and steel panel are created in ABAQUS with shell elements (S4R). Initial out-of-plane defects should be considered. In the modeling process, the buckling modes are calculated to extract the lowest buckling mode. Then, the "defect" command is used to modify the coordinates of the panel nodes based on buckling and the maximum out-of-plane deformation value is multiplied by it.

Boundary conditions and out-of-plane supports and constraints are considered similar to laboratory works [29]. The loading pattern consists of two stages: vertical loads and incremental lateral displacements. Cyclic structural model (composite hardening) is adopted to accurately simulate the behavior of steel, using ABAQUS material library of nonlinear kinematic hardening software. This model is parameterized in ABAQUS (Hardening = COMBINED model). Since the analysis of the thin steel plate shear wall under lateral loadings has severe nonlinear behaviors, including panel buckling, local column buckling, large out-of-plane deformation, and bidirectional tensile bands, the analyzes were performed with the nonlinear static module.

3. Research method

Steel shear wall with opening and pre-crack is evaluated in the present article in two parts. Since the finite element analysis of shear wall with opening and three-story frame is complicated and there is high probability of cracking, a numerical model is proposed to estimate the force-displacement response of SPSW. Using the presented idea, in the first step, cracks with a width of 10 mm and different lengths were created in the steel shear wall, and then in the second step, the push-over curve was obtained using the finite element method. There are various positions and combinations for cracking, which are shown below. As shown in Figure 4, this type of crack includes horizontal and vertical cracks in different positions of the steel frame filler plate. Critical cracks may occur in any position on the wall despite the openings, for this purpose, the composite of the position of more cracks in the tensile and compress field is considered.

4. Validation

In order to control and validate the behavior of the constructed finite element model, it is necessary to make a comparison between the results of the analytical and the laboratory model. The present study was conducted by numerical simulation using ABAQUS finite element simulator software. This comparison was made between the responses obtained from ABAQUS finite element modeling and Zhang et al.'s laboratory research [29].

In this article, a TM1 model, a three-story frame and a one-span steel shear wall presented by Zhang et al. is simulated with a center-to-center height of 2.05 ms and a thickness of 6 mm steel filler plate and different cross-sections of column beams as shown in Figure 2. The boundary members are made of ASTM-A572 steel, which is considered as a Tie constraint in welding modeling, and the filler sheet is made of steel with a yield point of 235 MPa. The schematic of the frame is shown in Figure 2. The type of element for steel shear wall modeling in ABAQUS finite element software is shell element.

The element used in boundary members (beam, column and support) and stiffeners and filler sheet, which is collectively called shear wall, is of S4R type. In order to achieve the appropriate mesh size, different dimensions have been selected for the

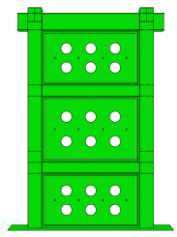
Crack with the length of 30 mm

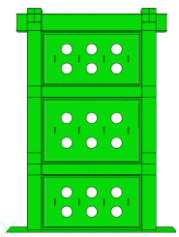
Crack with the length of 120 mm

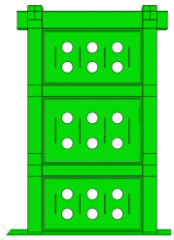
Crack with the length of 240 mm

(a): 4 vertical cracks in the middle of the shear wall, crack width 10 mm. (Group A)

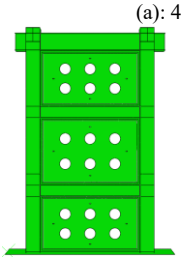
Crack with the length of 30 mm

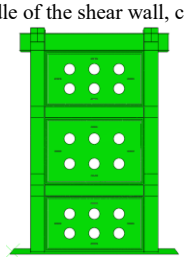
Crack with the length of 120 mm

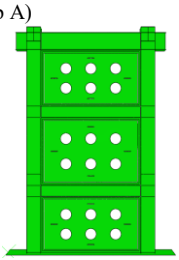
Crack with the length of 240 mm

(b): 4 horizontal cracks in the middle of the shear wall, crack width 10 mm. (Group H)

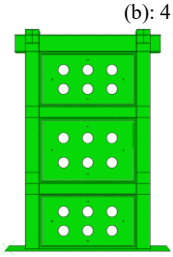
Crack with the length of 30 mm

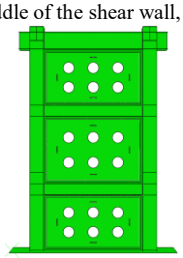
Crack with the length of 120 mm

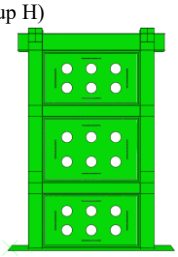
Crack with the length of 240 mm

(c): 4 horizontal-vertical cracks in the middle of the shear wall, crack width 10 mm. (Group R)

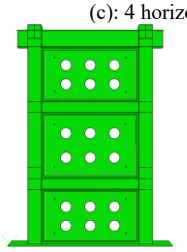
Crack with the length of 30 mm

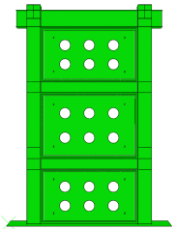
Crack with the length of 120 mm

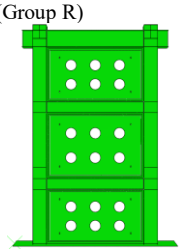
Crack with the length of 240 mm

(d): 4 vertical cracks in the corner of the shear wall, crack width 10 mm. (Group C)

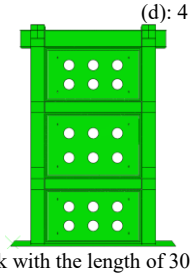
Crack with the length of 30 mm

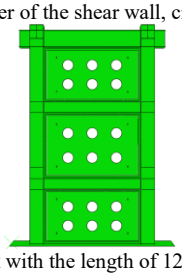
Crack with the length of 120 mm

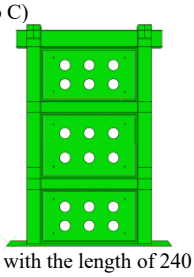
Crack with the length of 240 mm

(e): 4 horizontal cracks in the corner of the shear wall, crack width 10 mm. (Group D)

Figure 1- Crack position

elements, and by comparing and calibrating the numerical and laboratory results, the mesh size of 25 mm has been selected for the numerical samples, which has brought acceptable results.

The laboratory model of the shear wall investigated by Zhang et al. is shown in Figure 2 and the compared force-displacement diagram obtained from the laboratory results and modeling in ABAQUS software is shown in Figure 3. Figure 3 shows the force-displacement diagram obtained from the laboratory and the simulation results obtained from the finite element software, which has a slight difference with the laboratory results and is in good agreement with the laboratory results of Zhang et al. This comparison demonstrates the accuracy of the answers obtained from ABAQUS in the research and the accuracy of this software in modeling.

5. Parametric Study

In this study, steel shear walls with opening and pre-crack have been analyzed for axial and lateral compressive load. This study aims at investigating the lateral behavior of the shear wall of thin steel plate with pre-crack under lateral horizontal forces and at calculating the stiffness index, ultimate strength and ductility. The objective of the study is the shear panel with opening and pre-crack, on which the tensile fields of the adjacent panels above and below are applied. According to the applied engineering experience and published research, the selected size range of the thin steel sheet shear wall is as follows: the ratio of opening to height is about L/h = 1.5-2.0 and the ratio of height to thickness is about λ = 200-400. Based on these principles, 5 groups of pre-cracks were made in the three-story non-stiffened steel sheet shear wall sample. The steel sheet shear wall structure is generally composed of edge beams, edge columns, filler panels, beam-to-column connections, and opening plates. Welded steel frame is used as boundary members. The width of the plates connecting the shear sheet to the boundary members is 60 mm and its thickness is 8 mm. The capacity of the panels is calculated and designed by CAN/CSA-S16-01 and ANSI/AISC 341-05 standards.

Figure 2 - Shear wall modeling in Zhang et al.'s research

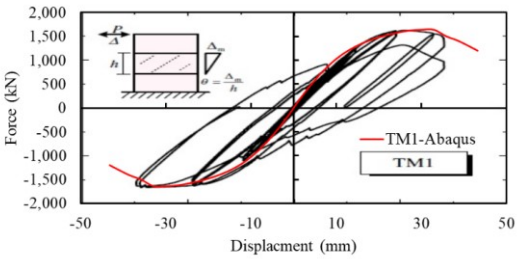

Figure 3 - Comparing the results of the force-displacement diagram in Zhang et al.'s research and Abaqus

Also, h_s is the central distance between the edge beams, I_c the bending stiffness of the edge column, Ls the central distance between the edge columns, A_c the area of the column, A_b the area of the beam and h the height of the panel.

$$\tan^4\alpha = \frac{1+\frac{L_s t_i}{2A_c}}{1+\frac{h_s t_i}{A_b}+\frac{{h_s}^4 t_i}{360 I_c L_s}}. \qquad M_u = \left(f_{py} t_i {h_s}^2 \sin^2\alpha\right)/12$$

$$V_u = 0.25 f_{py} t_i h_s \sin^2 2\alpha.$$

In the field of stiffness index, an approximate estimate has been reported in previous research, which used the initial slope of the force-displacement diagram and was used to calculate the ultimate strength and ductility indices from the maximum force and the ratio of the ultimate displacement to the yield displacement. In what follows, a detailed parametric study has been conducted to evaluate the pushover behavior of steel shear wall with pre-crack, for the parameters of pre-crack position, pre-crack length and the type of steel panel material. For the crack position parameter in group A, 4 vertical cracks in the middle of the shear wall, in group H 4 horizontal cracks in the middle of the shear wall, in group R 4 horizontal-vertical cracks in the middle of the shear wall, in group C 4 vertical cracks in the corner of the shear wall and in group D, 4 horizontal cracks in the corner of the shear wall are considered and the crack width is 10 mm in all models. For the crack length parameter, 30, 120 and 240 mm and for the material parameter of the steel panel LYP100, St37 and St52 are considered. The details of the numerical samples for the 48 studied frames are presented in Table 1.

6. Force-displacement Curves

In this part, the push-over behavior of pre-cracked steel shear wall with circular openings is compared. All the features of the steel frame and plate are similar for all samples. All samples were subjected to 3% circulation. The behavior of steel shear wall with circular openings in two rows of shear wall was considered. All models are divided into 3 groups, the first group is related to the position of the pre-crack, the second group to the length of the pre-crack, and the third group to the steel material of the filler sheet of the steel frame. The force-displacement diagrams for different modes of the parametric study are shown in Figures 4 to 6.

First, vertical loads were applied to the numerical specimens until the loads reached 500 kN. Using buckling analysis and the shape data of the first mode of the wall, small deformations outside the wall with a value of L/1500 were applied. No out-of-plane deformation was revealed in the specimens under examination until the time before yielding. With the increase in the lateral load, when the first elements reached the yield stress, out-of-plane deformation and buckling were observed around the cracks, and stress concentration was seen in the tensile bands and around the cracks. As the loading displacement increased, out-of-plane deformations and cross tensile bands were more and more evident. The filler panel entered the plastic stage earlier than the boundary members, which has fulfilled the principle of "strong frame and weak panel". During the period of below 1%, there is no buckling phenomenon. When the shear wall frame load reached 3Δy, instability and overall buckling occurred. This phenomenon was caused by the presence of pre-cracks and openings in the steel plate filling the frame. In the following, the effect of the parametric study on the lateral behavior and indices of the shear steel frame has been investigated.

6-1. The Impact of the Pre-break Position Parameter

In this part, the impact of the crack position on the lateral behavior of the shear wall has been investigated. In the figure, 9 curves are drawn, in each curve 5 graphs are drawn for 5 different modes of the pre-crack position. Numerical models, stiffness, ultimate strength and ductility indices have been compared. For modes of steel shear wall that has a 30 mm crack and different steel materials, the crack position parameter has no impact on the stiffness, ultimate strength, and ductility indices in each group, and the values of the indices and their percentage changes are given in Table 2. By changing the position of the crack in modes of steel shear wall that has a crack of 120 and 240 mm, the change in the position of the crack is more tangible.

The reduction of stiffness indices for the shear wall with different cracks and with LYP material has been achieved in the range of 14 to 22%, the ultimate strength index with the decreasing range of 8 to 15%, and the ductility with a decreasing trend of 12 to

Table 1. details of the numerical samples

No.	Name of sheer wall	Crack position	Crack length(mm)	Type of steel	No.	Name of sheer wall	Crack position	Crack length(mm)	Type of steel
1	DSW-N-0-LYP	-	0	LYP	25	DSW-R-120-ST37	R	120	ST37
2	DSW-A-30-LYP	A	30	LYP	26	DSW-R-240-ST37	R	240	ST37
3	DSW-A-120-LYP	A	120	LYP	27	DSW-C-30-ST37	C	30	ST37
4	DSW-A-240-LYP	A	240	LYP	28	DSW-C-120-ST37	C	120	ST37
5	DSW-H-30-LYP	H	30	LYP	29	DSW-C-240-ST37	C	240	ST37
6	DSW-H-120-LYP	H	120	LYP	30	DSW-D-30-ST37	D	30	ST37
7	DSW-H-240-LYP	H	240	LYP	31	DSW-D-120-ST37	D	120	ST37
8	DSW-R-30-LYP	R	30	LYP	32	DSW-D-240-ST37	D	240	ST37
9	DSW-R-120-LYP	R	120	LYP	33	DSW-N-0-ST52	-	0	ST52
10	DSW-R-240-LYP	R	240	LYP	34	DSW-A-30-ST52	A	30	ST52
11	DSW-C-30-LYP	C	30	LYP	35	DSW-A-120-ST52	A	120	ST52
12	DSW-C-120-LYP	C	120	LYP	36	DSW-A-240-ST52	A	240	ST52
13	DSW-C-240-LYP	C	240	LYP	37	DSW-H-30-ST52	H	30	ST52
14	DSW-D-30-LYP	D	30	LYP	38	DSW-H-120-ST52	H	120	ST52
15	DSW-D-120-LYP	D	120	LYP	39	DSW-H-240-ST52	H	240	ST52
16	DSW-D-240-LYP	D	240	LYP	40	DSW-R-30-ST52	R	30	ST52
17	DSW-N-0-ST37	-	0	ST37	41	DSW-R-120-ST52	R	120	ST52
18	DSW-A-30-ST37	A	30	ST37	42	DSW-R-240-ST52	R	240	ST52
19	DSW-A-120-ST37	A	120	ST37	43	DSW-C-30-ST52	C	30	ST52
20	DSW-A-240-ST37	A	240	ST37	44	DSW-C-120-ST52	C	120	ST52
21	DSW-H-30-ST37	H	30	ST37	45	DSW-C-240-ST52	C	240	ST52
22	DSW-H-120-ST37	H	120	ST37	46	DSW-D-30-ST52	D	30	ST52
23	DSW-H-240-ST37	H	240	ST37	47	DSW-D-120-ST52	D	120	ST52
24	DSW-R-30-ST37	R	30	ST37	48	DSW-D-240-ST52	D	240	ST52

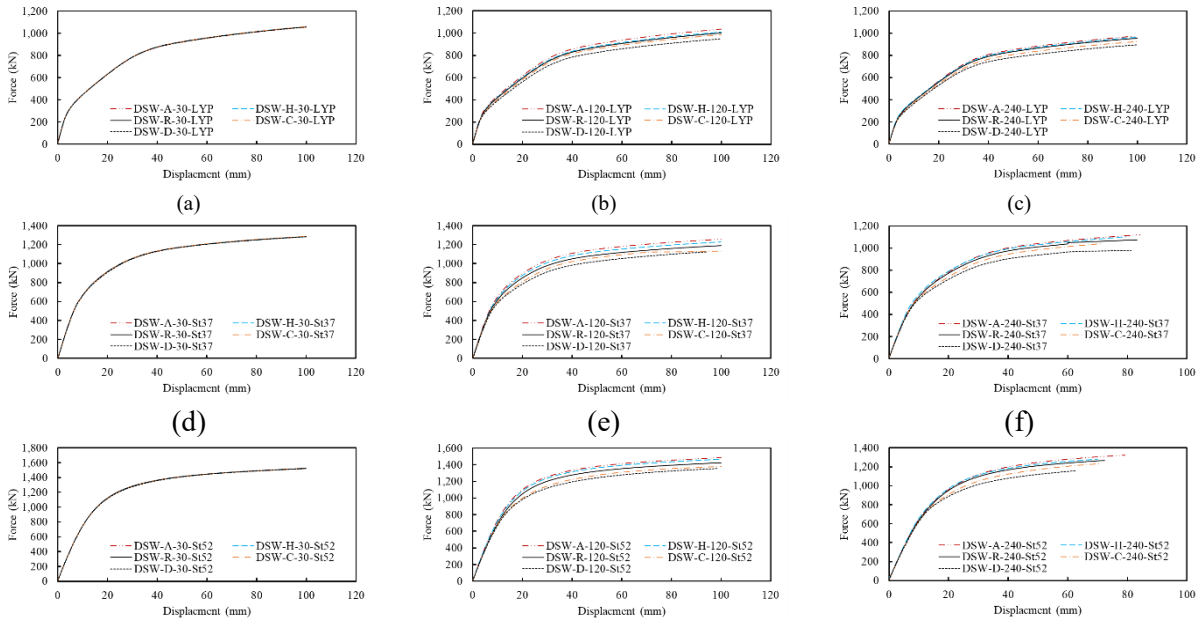

Figure 4 – Comparison of force-displacement curves for the pre-crack position

16%. This decrease in values also occurred due to the interruption of the tensile field of stress transfer in the shear wall. The decrease in strength can be clearly seen due to the breaking of the tensile bands around the cracks and the buckling phenomenon with the increase in displacement amplitude. Also, the increasing behavior of lateral load after yielding in the drawn diagrams is caused by the strain hardening behavior of steel materials. Table 1 shows the indices of yield strength, final consistency, stiffness and ductility of the samples. Ductility is one of the important indicators to evaluate the lateral performance of the structure. Displacement ductility factor can be calculated as the ratio of failure displacement to yield displacement. The results show that all samples have good ductility in the mode of cracks under 120 mm.

6-2. Effect of Crack Length in Shear Wall

In this part, the impact of the crack length in the shear wall on the lateral behavior of the shear wall has been investigated. In Figure 5, 15 curves are drawn, in each curve 4 graphs are drawn for 3 different modes of pre-crack length. In each group of steel shear walls, the position of the crack, the type of the fixed steel panel, and the length of the crack have been investigated in modes without cracks and with cracks of 30, 120, and 240 mm in length. Crack lengths of 120 and 240 mm have a significant effect on the distribution and transfer of stress in the tensile field, and the values of stiffness, ultimate strength and ductility indices and their percentage changes are given in Table 3. By changing the length of the crack in the modes of the steel shear wall that has the position of the crack C and D, there is a significant reduction in the structural indices of the wall. The reduction of stiffness indices for the shear wall with different crack positions and with LYP material has been achieved in the range of 20-50%, the ultimate strength index has decreased in the range of 4-16% and the ductility has been achieved with a decreasing trend of 28-51%. This decrease in values also occurred due to the interruption of the tensile field of stress transfer in the shear wall. The reduction of stiffness indices for the shear wall with different crack positions and with St37 material is in the range of 10 to 32%, the ultimate strength index is reduced in the range of 5 to 24%, and the ductility is also achieved with a decreasing trend of 28 to 60%. The reduction of stiffness indices for the shear wall with different crack positions and with St52 material has been achieved in the range of 8 to 35%, the ultimate strength index has decreased in the range of 2 to 24%, and the ductility has been achieved with a decreasing trend of 26 to 58%. The stiffness of the edge column has a great impact on the lateral bearing capacity of the shear wall structures, which are designed with high stiffness. Since the aim of steel panel research is pre-crack investigation, the results showed that the tensile fields are transferred to the edge beam and the effect of the tensile fields on the edge beam is compensated by the upper and lower adjacent panels. If the pre-cracks have a length of 240 mm, buckling failure occurs due to the interruption of the tensile field, the load-carrying capacity is greatly reduced and the energy dissipation capacity is lost, and this capacity intensification is more evident in the cracks in position C and D.

6-3. Impact of Shear Wall Steel Material

In this part, the impact of the steel material in the shear wall on the lateral behavior of the shear wall has been investigated. In Figure 6, 15 curves are drawn, in each curve 4 graphs are drawn for 3 different types of shear wall steel. In each group of steel shear walls, the crack position and fixed crack length and the steel material of the shear wall in LYP, St37 and St52 modes have been studied. The yield stress and final stress of different steels had a significant impact on the stress distribution in the tensile field and the values of the stiffness, ultimate strength and ductility indices and their percentage changes, which are given in Table 4. The increase in stiffness indices for the shear wall with St37 and St52 steel in the range of 2.53 to 3.63 times the stiffness of the LYP shear wall, the increased final strength index is equivalent to 1.1 to 1.45 times the strength of the LYP shear wall and the ductility has also been achieved with a decreasing trend of 8-30% compared to the shear wall with LYP material. This decrease in ductility values is achieved due to the high stiffness and strength of St37 and St52 steel materials compared to LYP steel.

6-4. Study on the Damage modes of Shear Wall with Pre-crack and Opening

In this part, the damage modes of the shear wall with pre-crack and opening for two types of cracks have been studied. Cumulative plastic strain (PEEQ) has been used to examine damage modes. This output shows the locations prone to crack growth and

Table 2 - Values of indices of steel shear wall with pre-crack

Shear wall name	Yield force (kN)	Stiffness (kN/mm)	Strength (kN)	Ductility	Shear wall name	Yield force (kN)	Stiffness (kN/mm)	Strength (kN)	Ductility	Shear wall name	Yield force (kN)	Stiffness (kN/mm)	Strength (kN)	Ductility
DSW-N-0-LYP	347.04	31.37	1058.99	9.04	DSW-N-0-St37	488.2	79.42	1286.39	8.3	DSW-N-0-St52	499.81	81.31	1523.85	7.81
DSW-A-30-LYP	427.98	25.49	1057.97	6.55	DSW-A-30-St37	600.82	71.56	1284.85	6.14	DSW-A-30-St52	617.06	73.5	1521.64	5.72
DSW-A-120-LYP	437.77	23.03	1035.52	5.79	DSW-A-120-St37	635.65	66.87	1256.46	5.47	DSW-A-120-St52	697.72	73.4	1487.82	5.05
DSW-A-240-LYP	351.83	21.88	975.89	5.47	DSW-A-240-St37	492.84	61.3	1119.58	4.48	DSW-A-240-St52	539.98	67.16	1320.94	4.18
DSW-H-30-LYP	463.97	23.48	1059.94	5.57	DSW-H-30-St37	664.08	67.21	1285.81	5.32	DSW-H-30-St52	732.68	74.15	1523.36	4.86
DSW-H-120-LYP	451.61	21.55	1011.37	5.25	DSW-H-120-St37	653.54	62.36	1226.57	4.96	DSW-H-120-St52	742.55	70.85	1467.45	4.58
DSW-H-240-LYP	321.58	19.36	964.49	4.97	DSW-H-240-St37	523.99	63.08	1101.32	4.28	DSW-H-240-St52	563.67	64.47	1314.94	3.99
DSW-R-30-LYP	463.14	23.28	1058.66	5.53	DSW-R-30-St37	666.48	67.01	1286.31	5.18	DSW-R-30-St52	742.03	74.6	1523.96	4.83
DSW-R-120-LYP	435.35	20.63	1001.62	5.21	DSW-R-120-St37	638.17	60.49	1190.75	4.93	DSW-R-120-St52	721.95	68.43	1424.32	4.55
DSW-R-240-LYP	267.19	17.95	954.49	5.02	DSW-R-240-St37	459.78	61.77	1074.33	4.71	DSW-R-240-St52	496.24	63.34	1298.75	4.39
DSW-C-30-LYP	456.07	23.74	1058.74	5.73	DSW-C-30-St37	649.16	67.58	1286.13	5.47	DSW-C-30-St52	718.64	74.81	1523.39	5
DSW-C-120-LYP	439.52	18.67	985.21	4.67	DSW-C-120-St37	649.87	55.21	1132.3	4.33	DSW-C-120-St52	748.56	63.59	1378.65	4.08
DSW-C-240-LYP	285.68	15.66	926.2	4.4	DSW-C-240-St37	517.99	56.8	1066.23	3.73	DSW-C-240-St52	573.72	55.99	1232.8	3.47
DSW-D-30-LYP	470.27	21.71	1057.7	5.08	DSW-D-30-St37	699.82	64.61	1285.77	4.8	DSW-D-30-St52	780.84	72.1	1522.99	4.43
DSW-D-120-LYP	424.26	18.82	950.46	4.88	DSW-D-120-St37	626.9	55.63	1123.66	4.57	DSW-D-120-St52	719.42	63.84	1339.87	4.26
DSW-D-240-LYP	331.42	16.89	894.75	4.48	DSW-D-240-St37	532.65	54.28	980.33	3.43	DSW-D-240-St52	613.38	53.13	1159.81	3.13

Table 3- The ratio of changes in steel shear wall indices with the change of pre-crack length

Shear wall name	Stiffness ratio	Strength ratio	Ductility ratio	Shear wall name	Stiffness ratio	Strength ratio	Ductility ratio
DSW-N-0-LYP	1	1	1	DSW-R-120-St37	0.76	0.93	0.59
DSW-A-30-LYP	0.81	1	0.72	DSW-R-240-St37	0.78	0.84	0.57
DSW-A-120-LYP	0.73	0.98	0.64	DSW-C-30-St37	0.95	1	0.66
DSW-A-240-LYP	0.7	0.92	0.61	DSW-C-120-St37	0.7	0.88	0.52
DSW-H-30-LYP	0.75	1	0.62	DSW-C-240-St37	0.72	0.83	0.45
DSW-H-120-LYP	0.69	0.96	0.58	DSW-D-30-St37	0.81	1	0.58
DSW-H-240-LYP	0.62	0.91	0.55	DSW-D-120-St37	0.7	0.87	0.55
DSW-R-30-LYP	0.74	1	0.61	DSW-D-240-St37	0.68	0.76	0.41
DSW-R-120-LYP	0.66	0.95	0.58	DSW-N-0-St52	1	1	1
DSW-R-240-LYP	0.57	0.9	0.56	DSW-A-30-St52	0.9	1	0.73
DSW-C-30-LYP	0.76	1	0.63	DSW-A-120-St52	0.9	0.98	0.65
DSW-C-120-LYP	0.6	0.93	0.52	DSW-A-240-St52	0.83	0.87	0.54
DSW-C-240-LYP	0.5	0.87	0.49	DSW-H-30-St52	0.91	1	0.62
DSW-D-30-LYP	0.69	1	0.56	DSW-H-120-St52	0.87	0.96	0.59
DSW-D-120-LYP	0.6	0.9	0.54	DSW-H-240-St52	0.79	0.86	0.51
DSW-D-240-LYP	0.54	0.84	0.5	DSW-R-30-St52	0.92	1	0.62
DSW-N-0-St37	1	1	1	DSW-R-120-St52	0.84	0.93	0.58
DSW-A-30-St37	0.9	1	0.74	DSW-R-240-St52	0.78	0.85	0.56
DSW-A-120-St37	0.84	0.98	0.66	DSW-C-30-St52	0.92	1	0.64
DSW-A-240-St37	0.77	0.87	0.54	DSW-C-120-St52	0.78	0.9	0.52
DSW-H-30-St37	0.85	1	0.64	DSW-C-240-St52	0.69	0.81	0.44
DSW-H-120-St37	0.79	0.95	0.6	DSW-D-30-St52	0.89	1	0.57
DSW-H-240-St37	0.79	0.86	0.52	DSW-D-120-St52	0.79	0.88	0.55
DSW-R-30-St37	0.84	1	0.62	DSW-D-240-St52	0.65	0.76	0.4

Table 4- The ratio of changes in the indices of steel shear wall with the change of steel type of steel sheet

Shear wall name	Stiffness ratio	Strength ratio	Ductility ratio	Shear wall name	Stiffness ratio	Strength ratio	Ductility ratio
DSW-N-0-LYP	1	1	1	DSW-R-120-LYP	1	1	1
DSW-N-0-St37	2.53	1.21	0.92	DSW-R-120-St37	2.93	1.19	0.95
DSW-N-0-St52	2.59	1.44	0.86	DSW-R-120-St52	3.32	1.42	0.87
DSW-A-30-LYP	1	1	1	DSW-R-240-LYP	1	1	1
DSW-A-30-St37	2.81	1.21	0.94	DSW-R-240-St37	3.44	1.13	0.94
DSW-A-30-St52	2.88	1.44	0.87	DSW-R-240-St52	3.53	1.36	0.87
DSW-A-120-LYP	1	1	1	DSW-C-30-LYP	1	1	1
DSW-A-120-St37	2.9	1.21	0.95	DSW-C-30-St37	2.85	1.21	0.96
DSW-A-120-St52	3.19	1.44	0.87	DSW-C-30-St52	3.15	1.44	0.87
DSW-A-240-LYP	1	1	1	DSW-C-120-LYP	1	1	1
DSW-A-240-St37	2.8	1.15	0.82	DSW-C-120-St37	2.96	1.15	0.93
DSW-A-240-St52	3.07	1.35	0.76	DSW-C-120-St52	3.41	1.4	0.87
DSW-H-30-LYP	1	1	1	DSW-C-240-LYP	1	1	1
DSW-H-30-St37	2.86	1.21	0.96	DSW-C-240-St37	3.63	1.15	0.85
DSW-H-30-St52	3.16	1.44	0.87	DSW-C-240-St52	3.57	1.33	0.79
DSW-H-120-LYP	1	1	1	DSW-D-30-LYP	1	1	1
DSW-H-120-St37	2.89	1.21	0.95	DSW-D-30-St37	2.98	1.22	0.95
DSW-H-120-St52	3.29	1.45	0.87	DSW-D-30-St52	3.32	1.44	0.87
DSW-H-240-LYP	1	1	1	DSW-D-120-LYP	1	1	1
DSW-H-240-St37	3.26	1.14	0.86	DSW-D-120-St37	2.96	1.18	0.94
DSW-H-240-St52	3.33	1.36	0.8	DSW-D-120-St52	3.39	1.41	0.87
DSW-R-30-LYP	1	1	1	DSW-D-240-LYP	1	1	1
DSW-R-30-St37	2.88	1.22	0.94	DSW-D-240-St37	3.21	1.1	0.76
DSW-R-30-St52	3.2	1.44	0.87	DSW-D-240-St52	3.15	1.3	0.7

damage in the shear wall as shown in Figures 7 and 8. The concentration distribution of plastic strain damage in the pre-cracks of the upright mode in the middle of the shear wall at the relative displacement angle of the filler sheet 0.5% has reached the plastic value and at the relative displacement angle of the boundary members the yield stress (von Mises) at 0.9%. First, the circulation occurred locally in the horizontal corrugated filler sheet with a circular opening and a pre-crack in the middle of the steel sheet and the corner of the pre-crack, and with the increase of the period of stress concentration and plastic strain in the upper and lower corners of these openings, and led to the growth of the circulation in the area around the opening and pre-cracks and local buckling have been created and yield stresses have developed in the beam and column members. And the progress of this circulation, has increased and turned

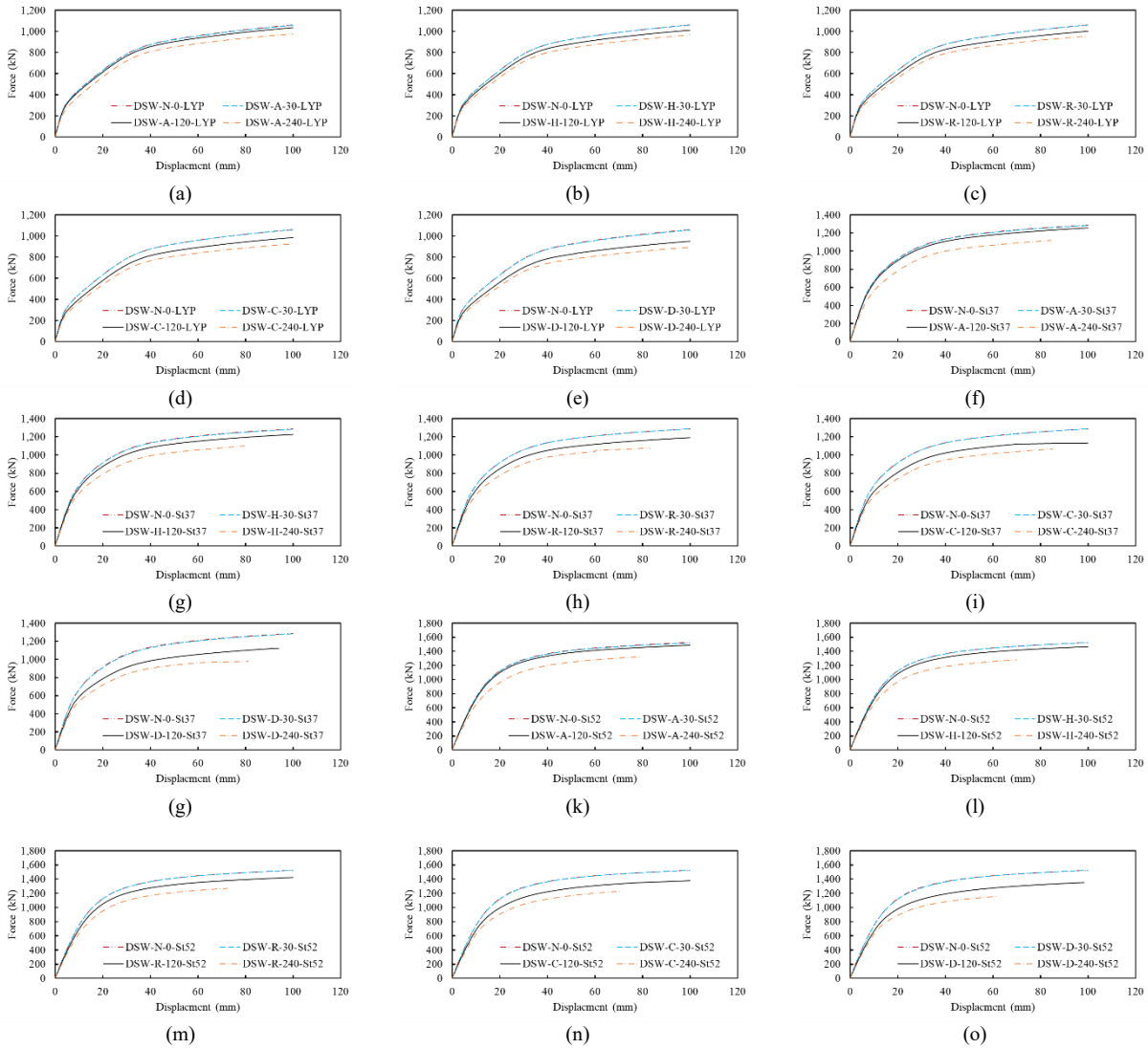

Figure 5 – Comparison of force-displacement curves for pre-crack length

into general buckling on the surface of the filler sheet, especially around the pre-cracks. An example of cumulative plastic strain and damage mode of the steel frame at 3% circulation is shown in Figures 7 and 8. The results of this study showed that the geometric stiffness and high resistance to general buckling and the concentration of buckling around the openings and pre-cracks depend on the position of the pre-crack and the tensile field of the wall. In general, cracks D and C with sizes of 120 and 240 mm have shown the most critical condition and the highest strain with values above 0.15, which means that the elements in this area are prone to the initiation of sheet tearing and crack growth.

7. Conclusion

In this article, 48 samples of steel sheet shear wall with circular opening and pre-crack with three-story frame and one opening were examined under axial and pushover loads to investigate the lateral behavior.

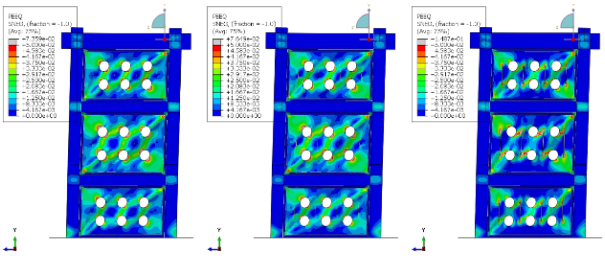

Figure 7 - Distribution of plastic strain damage concentration in the pre-cracks of the upright mode in the middle of the shear wall

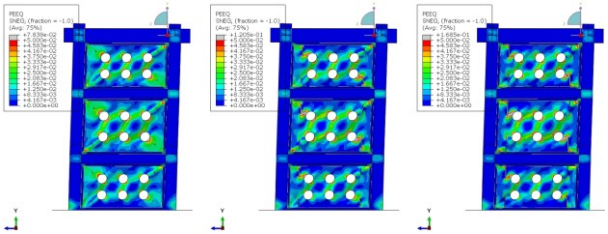

Figure 8 - Distribution of plastic strain damage concentration in the pre-cracks of the upright mode at the corner of the shear wall

The models made by the nonlinear finite element method of the steel sheet shear wall structure were confirmed with the test results.

Further, by examining the stiffness, resistance and ductility indicators of the wall, the following results were obtained:

Different steel sheet shear walls structures with opening and pre-crack for crack lengths of 120 to 240 mm showed low strength, stiffness and ductility, and the ductility coefficients were less than 5. The crack length and crack position parameters have a great impact on the ductility capacity, while they have little impact on the initial stiffness and strength. Horizontal cracks located at the top or bottom at the corners of the frame (positions C and D) had a great impact on the lateral behavior and reduced ductility by 60% and wall strength by 32%. Because these cracks cut the stress transmission path in the tensile field and the capacity of the wall is greatly reduced, in the mode of pre-crack with a length of 30 mm, the final strength of the wall did not change, but the stiffness and ductility decreased by 10 and 15%, respectively. By increasing the crack length from 30 to 120 mm, the ultimate strength, stiffness and ductility of the wall decreased by 6, 26 and 33%, respectively, and by changing the crack length from 30 to 240 mm, the ultimate strength, stiffness and ductility decreased by 11, 39 and 46%, respectively. Also, by changing the shear wall steel sheet material from LYP steel to St37 and St52, the ultimate strength and stiffness have increased by 3.63 and 1.45 times, respectively, and the ductility has decreased by 30%.

8. References

[1]. Thorburn, L. J., Montgomery, C. J., & Kulak, G. L. (1983). Analysis of steel plate shear walls.

[2]. Elgaaly, M., & Liu, Y. (1997). Analysis of thin-steel-plate shear walls. Journal of Structural Engineering, 123(11), 1487-1496.

[3]. Caccese, V., Elgaaly, M., & Chen, R. (1993). Experimental study of thin steel-plate shear walls under cyclic load. Journal of Structural Engineering, 119(2), 573-587.

[4]. Alavi, E., & Nateghi, F. (2009). Non-linear behavior and shear strength of diagonally stiffened steel plate shear walls. International Journal of Engineering, 22(4), 343-356.

[5]. Alinia, M. M., & Shirazi, R. S. (2009). On the design of stiffeners in steel plate shear walls. Journal of Constructional Steel Research, 65(10-11), 2069-2077.

[6]. Driver, R. G., Kulak, G. L., Kennedy, D. L., & Elwi, A. E. (1998). Cyclic test of four-story steel plate shear wall. Journal of Structural Engineering, 124(2), 112-120.

[7]. Guo, H. C., Hao, J. P., & Liu, Y. H. (2015). Behavior of stiffened and unstiffened steel plate shear walls considering joint properties. Thin-Walled Structures, 97, 53-62.

[8]. Sigariyazd, M. A., Joghataie, A., & Attari, N. K. (2016). Analysis and design recommendations for diagonally stiffened steel plate shear walls. Thin-Walled Structures, 103, 72-80.

[9]. Alavi, E., & Nateghi, F. (2013). Experimental study on diagonally stiffened steel plate shear walls with central perforation. Journal of Constructional Steel Research, 89, 9-20.

[10]. Alavi, E., & Nateghi, F. (2013). Experimental study of diagonally stiffened steel plate shear walls. Journal of Structural Engineering, 139(11), 1795-1811.

[11]. Du, Y., Hao, J., Yu, J., Yu, H., Deng, B., Lv, D., & Liang, Z. (2018). Seismic performance of a repaired thin steel plate shear wall structure. Journal of Constructional Steel Research, 151, 194-203.

[12]. Xu, L., Liu, J., & Li, Z. (2021). Parametric analysis and failure mode of steel plate shear wall with self-centering braces. Engineering Structures, 237, 112151.
[13]. Tong, J. Z., & Guo, Y. L. (2015). Elastic buckling behavior of steel trapezoidal corrugated shear walls with vertical stiffeners. Thin-Walled Structures, 95, 31-39.
[14]. Xu, Z., Tong, G., & Zhang, L. (2018). Elastic and elastic-plastic threshold stiffness of stiffened steel plate walls in compression. Journal of Constructional Steel Research, 148, 138-153.
[15]. Gen-shu, T. O. N. G., & Wen-deng, T. A. O. (2013). Elastic shear buckling of steel shear walls strengthened vertically by closed section stiffeners. 30(9), 1-9.
[16]. Nie, J. G., Zhu, L., Fan, J. S., & Mo, Y. L. (2013). Lateral resistance capacity of stiffened steel plate shear walls. Thin-Walled Structures, 67, 155-167.
[17]. Hosseinzadeh, S. A. A., & Tehranizadeh, M. (2012). Introduction of stiffened large rectangular openings in steel plate shear walls. Journal of Constructional Steel Research, 77, 180-192.
[18]. Sabouri-Ghomi, S., & Mamazizi, S. (2015). Experimental investigation on stiffened steel plate shear walls with two rectangular openings. Thin-Walled Structures, 86, 56-66.
[19]. Shekastehband, B., Azaraxsh, A., & Showkati, H. (2017). Experimental and numerical study on seismic behavior of LYS and HYS steel plate shear walls connected to frame beams only. Archives of civil and mechanical engineering, 17(1), 154-168.
[20]. Berman, J. W., & Bruneau, M. (2005). Experimental investigation of light-gauge steel plate shear walls. Journal of Structural Engineering, 131(2), 259-267.
[21]. Vian, D., Bruneau, M., & Purba, R. (2009). Special perforated steel plate shear walls with reduced beam section anchor beams. II: Analysis and design recommendations. Journal of Structural Engineering, 135(3), 221-228.
[22]. Purba, R., & Bruneau, M. (2009). Finite-element investigation and design recommendations for perforated steel plate shear walls. Journal of structural engineering, 135(11), 1367-1376.
[23]. Purba, R., & Bruneau, M. (2009). Finite-element investigation and design recommendations for perforated steel plate shear walls. Journal of structural engineering, 135(11), 1367-1376.
[24]. Guo, L., Rong, Q., Ma, X., & Zhang, S. (2011). Behavior of steel plate shear wall connected to frame beams only. International Journal of Steel Structures, 11(4), 467-479.
[25]. Vatansever, C., & Yardimci, N. (2011). Experimental investigation of thin steel plate shear walls with different infill-to-boundary frame connections. Steel and Composite Structures, 11(3), 251-271.
[26]. Shekastehband, B., Azaraxsh, A. A., Showkati, H., & Pavir, A. (2017). Behavior of semi-supported steel shear walls: Experimental and numerical simulations. Engineering structures, 135, 161-176.
[27]. Wei, M. W., Liew, J. R., Yong, D., & Fu, X. Y. (2017). Experimental and numerical investigation of novel partially connected steel plate shear walls. Journal of Constructional Steel Research, 132, 1-15.
[28]. Documentation, A., & Manual, U. (2010). Version 6.14. Dassault systemes.
[29]. Wang, M., Shi, Y., Xu, J., Yang, W., & Li, Y. (2015). Experimental and numerical study of unstiffened steel plate shear wall structures. Journal of Constructional Steel Research, 112, 373-386.